Synthesis, crystal structure, and magnetism of the binuclear radical complex [N-hydrogenpyridinium]$_2$[Ni(tdas)$_2$]$_2$

Chi-Feng Wang, Fang Qiao, Yan-Hui Chi, Jing-Min Shi, Ethan Cottrill, Ning Pan, Wei-Wei Zhu-ge, Yong-Xin Fu, Jun Xu & Xiao-Ping Qian

➕ View supplementary material ⬈

📅 Published online: 25 Sep 2015.

✏️ Submit your article to this journal ⬈

📊 Article views: 40

🔍 View related articles ⬈

☑️ View Crossmark data ⬈

Taylor & Francis
Taylor & Francis Group

Synthesis, crystal structure, and magnetism of the binuclear radical complex [N-hydrogenpyridinium]2[Ni(tdas)2]2

CHI-FENG WANG†, FANG QIAO†, YAN-HUI CHI*†, JING-MIN SHI†*, ETHAN COTTRILL‡, NING PAN†, WEI-WEI ZHU-GE†, YONG-XIN FU†, JUN XU† and XIAO-PING QIAN†

†College of Chemistry, Chemical Engineering and Materials Science, Collaborative Innovation Center of Functionalized Probes for Chemical Imaging in Universities of Shandong, Key Laboratory of Molecular and Nano Probes, Ministry of Education, Shandong Provincial Key Laboratory of CleanProduction of Fine Chemicals, Shandong Normal University, Jinan, PR China
‡Department of Chemistry and Biochemistry, Center for Intelligent Chemical Instrumentation, Ohio University, Athens, OH, USA
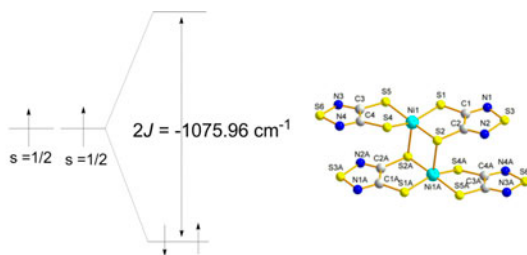
The binuclear radical complex [N-hydrogenpyridinium]2[Ni(tdas)2]2 (tdas = 1,2,5-thiazole-3,4-dithiolate) has been prepared and its crystal structure determined by X-ray crystallography. In the binuclear radical complex, the two nickel ions assume a distorted pyramidal geometry and are bridged by two sulfurs of different tdas anionic ligands. ESR spectra and the theoretical calculations reveal a very strong antiferromagnetic interaction in the binuclear radical complex, leading to diamagnetic crystals. The theoretical calculations also reveal a very weak antiferromagnetic interaction between adjacent radical complexes. This study is the first to report the magnetism of a binuclear radical nickel complex with tdas as ligand.

1. Introduction

For more than seven decades, molecular magnetism has been intensively studied [1–7] in order to prepare molecule-based devices and to understand electron transfer mechanisms.

---

*Corresponding authors. Email: xjonly@sdnu.edu.cn

Radical complexes display interesting magnetic coupling properties, especially for complexes with maleonitriledithiolate (mnt) [8–11] and 1,3-dithiole-2-thione-4,5-dithiolate (dmit) [12–14] as ligands and nickel, palladium and platinum as central ions. Some of these complexes exhibit strong intermolecular magnetic interactions while others display spin transitions [12, 15–18], which are attributes of molecular switches and may lead to utilization in molecular electronics for memory or sensing applications. Structurally, 1,2,5-thiazole-3,4-dithiolate (tdas) is similar to mnt and dmit, which suggests that it may be used to prepare analogous radical complexes. Compared with dmit or mnt, only limited complexes with tdas as ligand have been reported [19–29], from which only one anionic radical mononuclear nickel complex has been studied and its magnetism reported [30]. Magnetic coupling properties of binuclear nickel complexes are dependent on their bridging mode, the coordination geometry of the nickel ion, and other electronic and structural factors. For example, some binuclear nickel complexes [7, 31, 32] with octahedral coordination geometry and chloride, bromide, thiocyanate, selenocyanate, and azide as bridging ligands display ferromagnetic coupling interactions, whereas others [32–34] exhibit antiferromagnetic interactions. Herein, in order to understand the magnetic coupling properties of radical complexes with tdas as ligand and to further understand the differences in the magnetic coupling properties between radical and non-radical binuclear nickel complexes, we report the synthesis, crystal structure, and magnetism of the title complex.

2. Experimental

2.1. *Materials*

Na_2tdas [23] and N-hydrogenpyridium bromide [35] were prepared according to the literature. All other chemicals were analytical grade and used without purification.

2.2. *Preparation of complex*

2.2.1. Preparation of complex [N-hydrogenpyridinium]$_2$[Ni(tdas)$_2$]. A 5 mL water solution of $NiCl_2 \cdot 6H_2O$ (0.5950 g, 2.50 mM) was added into 10 mL methanol solution of Na_2tdas (0.9710 g, 5.00 mM), and the solution was stirred for one hour. The solution above was then added into 10 mL water solution of N-hydrogenpyridinium bromide (0.8000 g, 5.00 mM), and the mixture was stirred for ten minutes, during which a brownish sediment appeared. Brownish microcrystals were obtained after recrystallization of the brownish sediment from diethyl ether.

2.2.2. Preparation of complex [N-hydrogenpyridinium]$_2$[Ni(tdas)$_2$]$_2$. A 20 mL acetone solution of iodine (0.1270 g, 0.50 mM) was added into 180 mL of a mixed solution of acetone (150 mL) and methanol (30 mL) containing [N-hydrogenpyridinium]$_2$[Ni(tdas)$_2$] (0.5150 g, 1.00 mM), and the mixed solution was stirred for ten minutes and then filtered. Deep brown single crystals were obtained after the filtrate was allowed to stand and slowly evaporate at room temperature for one week. IR (cm^{-1}): 1740(w), 1622(w), 1475(w), 1387 (w), 1235(m), 789(m), 743(s), 670(s), 493(s). Elemental anal. Calcd for $C_9H_6N_5NiS_6$ (FW 435.26): C, 24.83; H, 1.39; N, 16.09; Ni, 13.48%. Found: C, 24.53; H, 1.65; N, 16.38; Ni, 13.89%.

2.3. *Physical measurements*

Infrared spectra were recorded with a Bruker Tensor 27 infrared spectrometer from 4000 to 500 cm^{-1} with KBr disks. C, H, and N elemental analyses were carried out on a Perkin–Elmer 2400 instrument, and Ni content was measured on an atomic spectrophotometer model Z-8000. X-band ESR spectra in solid and acetonitrile solution were recorded on an electron spin resonance spectrometer model Bruker A300.

2.4. *X-ray crystallography*

An intense brown single crystal with dimensions of $0.20 \times 0.14 \times 0.10$ mm was selected and glued to the tip of a glass fiber. The crystal structure determination was carried out at 25 °C on an X-ray diffractometer, Model Agilent SuperNova CCD, using graphite monochromated CuKα radiation ($\lambda = 1.54184$ Å) in the range of $8.32° < 2\theta < 141.82°$. A total of 5311 reflections were collected, of which 2778 were independent ($R_{int} = 0.0313$), and 2283 observed reflections with $I > 2\sigma(I)$ were used in the structure analysis. Corrections for Lp factors were applied, and all non-hydrogen atoms were refined with anisotropic thermal parameters. All hydrogens were placed in the calculated positions and refined as riding. The programs for structure solution and refinement were SHELXTL (Bruker, 2001) and SHELXTL. The pertinent crystallographic data and structural refinement parameters are summarized in table 1.

2.5. *Computational details*

All calculations are based on the models (figures 1 and 2), in which the bond length data, the associated angles, and the relevant locations of adjacent complexes were taken from the X-ray structures of the crystal.

The overlap integrals of the SOMOs were obtained using the orbital analysis. The calculations were performed using the Gaussian 03 program package [36] at the B3LYP level of theory, using the def2-TZVP basis set for all atoms. The detailed data of the spin densities and the overlap integrals of the calculated models are provided in tables 2–5.

The magnetic coupling constants of the models were studied using density functional theory with the broken-symmetry approach (BS) [37–39]. The exchange coupling constants J have been evaluated by calculating the energy difference between the high-spin state (E_{HS}) and the broken-symmetry state (E_{BS}). Assuming the spin Hamiltonian is defined as:

Table 1.   Crystallographic data of the title complex.

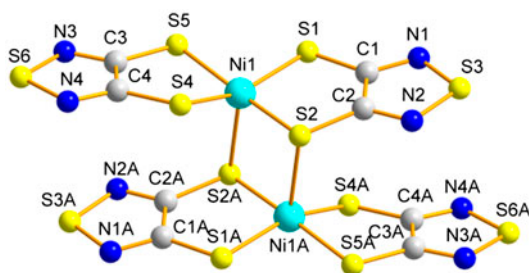|	
Formula	$C_9H_6N_5NiS_6$
Crystal system	Monoclinic
Space group	*C*2/*c*
a (Å)	18.9844(9)
b (Å)	13.8453(5)
c (Å)	12.8906(5)
β (°)	119.343(4)
V (Å^3), *Z*	2953.5(2), 8
Dc (g cm^{-1})	1.958
μ (mm^{-1})	9.821
R_1 [$I > 2\sigma(I)$]	0.0435
GOF	1.062
$(\Delta\rho)_{Max}$ (e Å^{-3})	0.676
$(\Delta\rho)_{Min}$ (e Å^{-3})	−0.601

Figure 1.   Model 1 for the magnetic interaction of the binuclear radical complex.
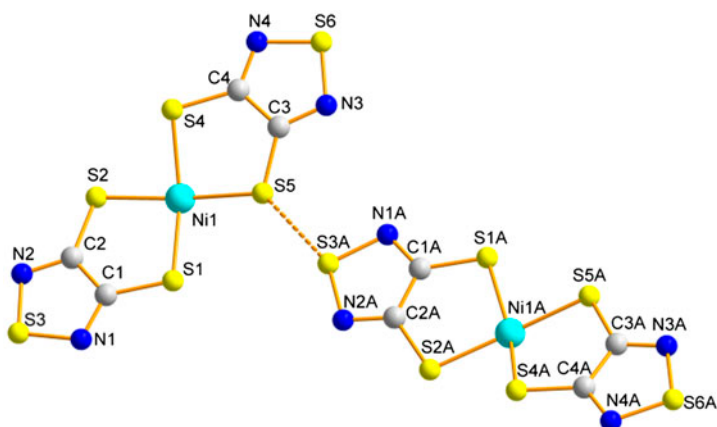

Figure 2.   Model 2 for the magnetic interaction between the adjacent binuclear radical complexes.

Table 2.   The spin density values for Model 1.

Atom	Spin density	Atom	Spin density
C1	0.004368	C1A	0.004368
C2	−0.021981	C2A	−0.021981
C3	−0.007405	C3A	−0.007405
C4	−0.010041	C4A	−0.010041
N1	−0.004248	N1A	−0.004248
N2	0.034970	N2A	0.034970
N3	0.010626	N3A	0.010626
N4	0.010319	N4A	0.010319
Ni1	0.709571	Ni1A	0.709571
S1	0.013154	S1A	0.013154
S2	0.170809	S2A	0.170809
S3	0.028206	S3A	0.028206
S4	0.016246	S4A	0.016246
S5	0.013583	S5A	0.013583
S6	0.031823	S6A	0.031823

Table 3.   The spin density values for Model 2.

Atom	Spin density	Atom	Spin density
C1	−0.017355	C1A	−0.013723
C2	−0.007598	C2A	−0.001875
C3	−0.007944	C3A	−0.008605
C4	−0.011708	C4A	−0.011233
N1	0.017428	N1A	0.011516
N2	0.005762	N2A	0.001222
N3	0.005762	N3A	0.009825
N4	0.009776	N4A	0.010823
Ni1	0.605123	Ni1A	0.544786
S1	0.109836	S1A	0.150088
S2	0.049115	S2A	0.083309
S3	0.048388	S3A	0.074089
S4	0.092205	S4A	0.073333
S5	0.052606	S5A	0.040378
S6	0.045457	S6A	0.035289

Table 4.   The overlap integrals between bridging atoms for Model 1.

Bond atoms	SOMO 1	SOMO 2
Ni1–S2A	0.0005	0.0035
Ni1A–S2	0.0005	0.0035

Table 5.   The overlap integral between the short contact atoms for Model 2.

Model	SOMO 1	SOMO 2
S5···S3A	−0.0003	−0.0006

$$\hat{H} = -2J\hat{S}_1 \cdot \hat{S}_2 \tag{1}$$

with $\hat{S}_1 = \hat{S}_2 = \frac{1}{2}$, the J value between two radical anionic transition metal complexes was obtained from equation (2), which was proposed by Noodleman [37–39]:

$$J = \frac{E_{BS} - E_{HS}}{S_{Max}^2} \tag{2}$$

in which S_{Max} is 1. To obtain exchange coupling constants J, Orca 2.8.0 calculations [40] were performed with the B3LYP level of theory as proposed by Becke [41, 42] and Lee et al. [43], which can provide J values in agreement with the experimental data for transition metal complexes. The def2-TZVP basis set [44, 45] as proposed by Ahlrichs and co-workers was used for all atoms in our calculations. Strong convergence criteria were used in order to ensure that the results are well converged with respect to technical parameters (the system energy was set to be smaller than 10^{-7} Hartree).

3. Results and discussion

3.1. *Crystal structure*

Figure 3 displays the crystal structure of [N-hydrogenpyridinium]$_2$[Ni(tdas)$_2$]$_2$ at 288 K, and table 6 provides data of the relevant coordination bond lengths and associated angles. From figure 3 and table 6, Ni1 is coordinated by three tdas ligands and the bond lengths range from 2.2147(11) to 2.3894(10) Å with the associated angles changing from 83.85(4)° to 173.98(4)°. Each Ni assumes a distorted square pyramidal geometry, coinciding with the reported anionic radical complex $\left[\text{Ni(tdas)}_2\right]_2^{2-}$ [26, 30]. The S2 and S2A function as bridges and coordinate two Ni ions with separation of 3.1710 Å, resulting in the formation of a binuclear complex which is nearly identical with the reported [PBu$_4$][Ni(tdas)$_2$] [26]. In the crystal, each binuclear complex links with four other binuclear radical complexes via intermolecular S···S short contacts, as shown in figure 4, in which the separation of the S···S is 3.4998(15) Å.

3.2. *Magnetic study*

Figure 5 shows the ESR spectrum of the complex in polycrystalline powder at room temperature. As observed, there is no ESR signal in the polycrystalline powder. The ESR silence in the solid implies that there is a strong antiferromagnetic interaction within the binuclear radical complex [26, 46].

In order to further understand the magnetic coupling information, theoretical calculations were performed. In the crystal, the magnetic interactions mainly come from two channels: (1) the magnetic interaction within the binuclear complex through the bridged sulfurs and (2) the magnetic interaction between the adjacent complexes, as shown in figures 1 and 2, respectively. Therefore, theoretical calculations were based on Models 1 and 2. The theoretical calculations reveal that the magnetic interaction of Model 1 is as strong as
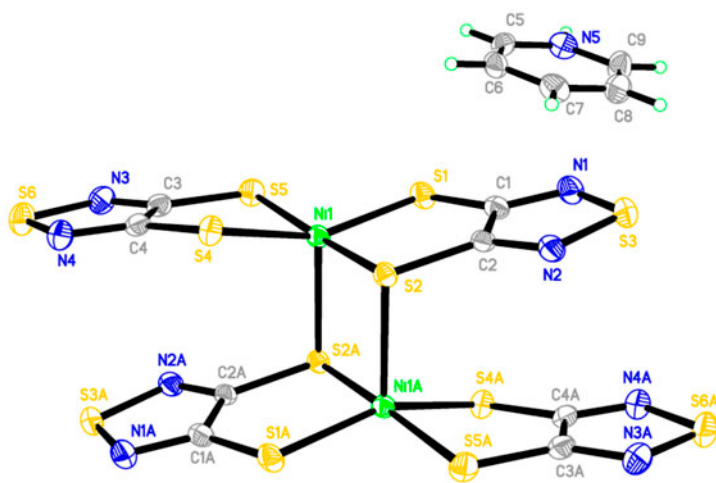

Figure 3. Crystal structure of the binuclear radical anion $\left[\text{Ni(tdas)}_2\right]_2^{2-}$ and counter-cation [N-hydrogenpyridinium]$^+$.

Table 6.   Selected bond lengths (Å) and angles (°).

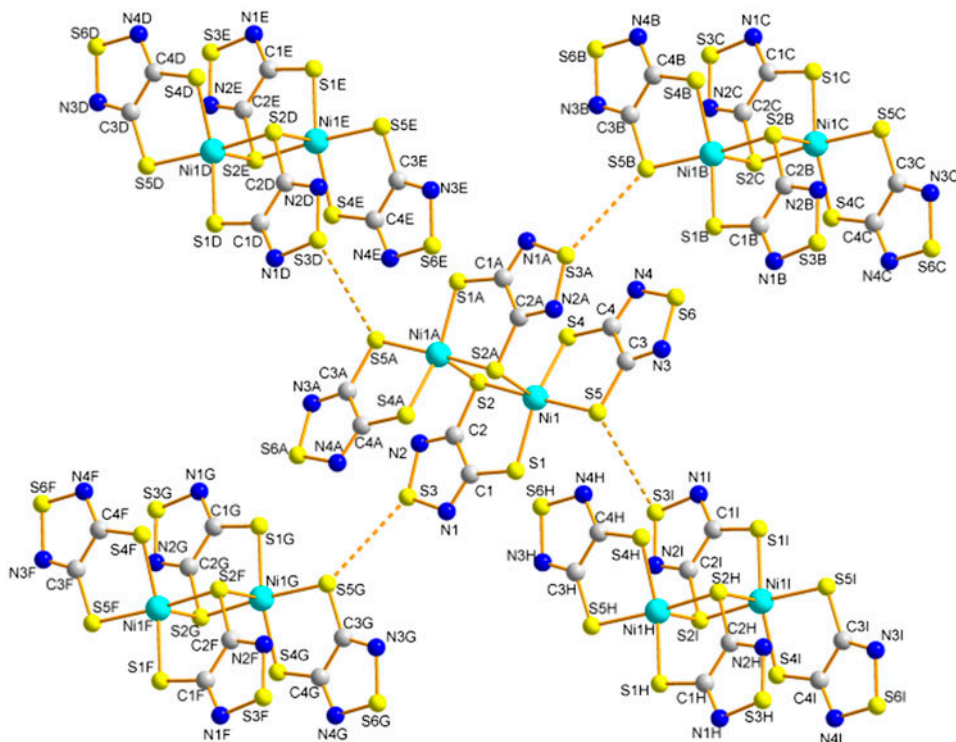| Ni1–S1	2.2353(11)	Ni1–S2	2.2147(11)	Ni1–S4	2.2328(11)
Ni1–S5	2.2438(11)	Ni1–S2A	2.3894(10)		
S2–Ni1–S1	93.46(4)	S2–Ni1–S4	83.85(4)	S4–Ni1–S5	91.85(4)
S1–Ni1–S5	88.83(4)	S4–Ni1–S1	156.75(5)	S2–Ni1–S5	173.98(4)
S1–Ni1–S2A	97.39(4)	S2–Ni1–S2A	93.02(4)	S4–Ni1–S2A	105.81(4)
S5–Ni1–S2A	92.20(4)				

Figure 4.   The intermolecular interaction (dashed line) between the adjacent binuclear complexes.

$2J = -1075.96$ cm^{-1}, whereas the magnetic interaction of Model 2 is only $2J = -0.22$ cm^{-1}. The theoretical calculations indicate that the strong antiferromagnetic coupling strength comes from the binuclear radical complex, which led to the diamagnetism and ESR silence. The very weak antiferromagnetic interaction from the theoretical calculations for Model 2 is close to the reported experimental value [28], which comes from similar intermolecular interactions. Tables 2–5 provide the data of the related spin density and overlap integral values for Models 1 and 2. These data clearly reveal strong antiferromagnetic coupling strength of Model 1 should be attributed to the large spin densities [47] on the bridging Ni1, Ni1A, S2, and S2A, as well as the large overlap integrals between them. In Model 2, the spin densities on the short contact atoms S5 and S3A are smaller than 0.1 and the related overlap integrals are far smaller than those of Model 1. Therefore, the very weak antiferromagnetic interaction for Model 2 should be attributed to the smaller spin
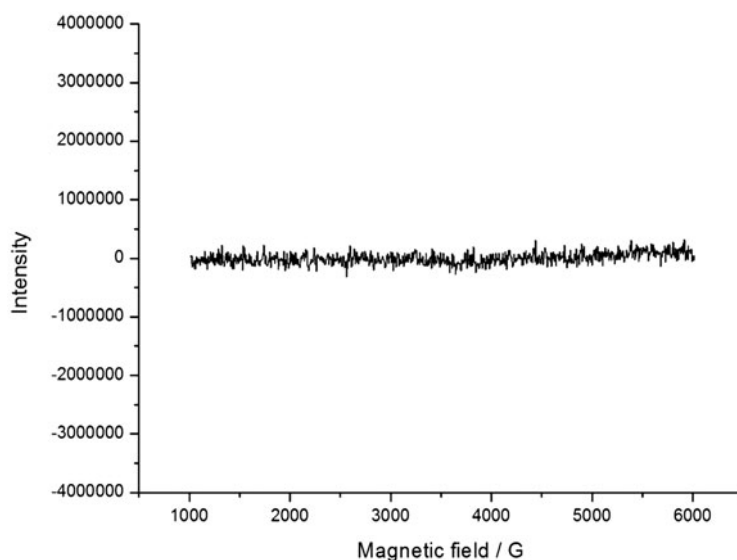
Figure 5.   ESR spectrum of the title complex in polycrystalline powder at room temperature.

densities [47] on the short contact atoms S5 and S3A and the smaller overlap integrals between them. In addition, the strong antiferromagnetic coupling of the present complex differentiates it from reported non-radical binuclear complexes [7, 31–34]. This distinction may be explained by the fact that the present complex is a radical binuclear nickel complex, whereas the reported ones [7, 31–34] are non-radical binuclear nickel complexes, as well as by differences in the coordination geometries and bridging ligands.

4. Conclusion

A radical binuclear nickel complex with tdas as ligand was prepared and its magnetic coupling interaction studied through ESR spectra and theoretical calculations. The strong antiferromagnetic interaction in the binuclear complex is attributed to the larger spin densities on the bridging atoms and the larger related overlap integrals, whereas the very weak antiferromagnetic interaction between the adjacent binuclear complexes is attributed to the smaller spin densities on the short contact atoms and the related smaller overlap integrals. Strong antiferromagnetic interaction of the present radical binuclear nickel complex differentiates it from the reported non-radical binuclear nickel complexes; this distinction is primarily ascribed to the radical nature of the present complex, as well as by differences in the coordination geometries and bridging ligands. This study helps to elucidate the magnetic coupling mechanism of anionic radical complexes with tdas as ligand and understand the differences in the magnetic coupling properties between radical and non-radical binuclear nickel complexes, thereby providing insight into preparing new molecular magnetic materials.

Supplementary material

CCDC 1032145 contains detailed information of the crystallographic data for this article. These data can be obtained free of charge from the Cambridge Crystallographic Data Center via http://www.ccdc.cam.ac.uk/data_request/cif.

Acknowledgements

Disclosure statement

No potential conflict of interest was reported by the authors.

Supplemental data

Supplemental data for this article can be accessed at http://dx.doi.org/10.1080/00958972.2015.1084417.

References

[1] J.P. Malrieu, R. Caballol, C.J. Calzado, C. de Graaf, N. Guihéry. *Chem. Rev.*, **114**, 429 (2014).
[2] H.-N. Li, R.-Z. Wei, Y.-H. Chi, W. Wei, H. Du, S.-G. Zhang, J.-M. Shi. *J. Coord. Chem.*, **66**, 3063 (2013).
[3] P. Wang, Y.-Y. Wang, Y.-H. Chi, W. Wei, S.-G. Zhang, E. Cottrill, J.-M. Shi. *J. Coord. Chem.*, **66**, 3092 (2013).
[4] R.-Z. Wei, J.-M. Shi, W. Wei, S.-L. Liu. *J. Coord. Chem.*, **66**, 1916 (2013).
[5] Y.-Y. Wang, Q.-H. Liu, W. Wei, H. Du, J.-M. Shi, Y.-Q. Zhang. *J. Coord. Chem.*, **66**, 254 (2013).
[6] Y. Journaux, O. Kahn. *J. Chem. Soc., Dalton Trans.*, 1575 (1979).
[7] A.P. Ginsberg, R.L. Martin, R.W. Brookes, R.C. Sherwood. *Inorg. Chem.*, **11**, 2884 (1972).
[8] W.-B. Pei, J.-S. Wu, X.-M. Ren, Z.-F. Tian, J.-L. Xie. *Dalton Trans.*, **41**, 2667 (2012).
[9] W.-B. Pei, J.-S. Wu, Z.-F. Tian, X.-M. Ren, Y. Song. *Inorg. Chem.*, **50**, 3970 (2011).
[10] X.-M. Ren, S. Nishihara, T. Akutagawa, S. Noro, T. Nakamura, W. Fujita, K. Awaga. *Chem. Phys. Lett.*, **418**, 423 (2006).
[11] Y. Hou, C.-L. Ni, J.-R. Zhou, X.-P. Liu, L.-L. Yu, L.-M. Yang. *Synth. Met.*, **158**, 379 (2008).
[12] O. Jeannin, R. Clérac, M. Fourmigué. *Cryst. Eng. Comm.*, **9**, 488 (2007).
[13] T. Kusamoto, H.M. Yamamoto, N. Tajima, Y. Oshima, S. Yamashita, R. Kato. *Inorg. Chem.*, **51**, 11645 (2012).
[14] N. Hoshino, K. Kubo, T. Nakamura, T. Akutagawa. *Dalton Trans.*, **41**, 9297 (2012).
[15] S.-Q. Zang, X.-M. Ren, Y. Su, Y. Song, W.-J. Tong, Z.-P. Ni, H.-H. Zhao, S. Gao, Q.-J. Meng. *Inorg. Chem.*, **48**, 9623 (2009).
[16] X.-M. Ren, S. Nishhara, T. Akutagawa, S. Noro, T. Nakamura, W. Fujita, K. Awaga, Z.-P. Ni, J.-L. Xie, Q.-J. Meng, R.K. Kremer. *Dalton Trans.*, 1988 (2006).
[17] X.-M. Ren, Q.-J. Meng, Y. Song, C.-S. Lu, C.-J. Hu. *Inorg. Chem.*, **41**, 5686 (2002).
[18] C.-L. Ni, D.-B. Dang, Y.-Z. Li, Z.-R. Yuan, Z.-P. Ni, Z.-F. Tian, Q.-J. Meng. *Inorg. Chem. Commun.*, **7**, 1034 (2004).
[19] A. Alberola, R. Llusar, S. Triguero, C. Vicent, M.N. Sokolov, C. Gómez-García. *J. Mater. Chem.*, **17**, 3440 (2007).

[20] N. Robertson, K. Awaga, S. Parsons, A. Kobayashi, A.E. Underhill. *Adv. Mater. Opt. Electron.*, **8**, 93 (1998).

[21] C.-L. Ni, D.-B. Dang, Z.-P. Ni, Y.-Z. Li, J.-L. Xie, Q.-J. Meng, Y.-G. Yao. *J. Coord. Chem.*, **57**, 1529 (2004).

[22] T. Okuno, K. Kuwamoto, W. Fujita, K. Awaga, W. Nakanishi. *Polyhedron*, **22**, 2311 (2003).

[23] D. Simão, H. Alves, I.C. Santos, V. Gama, M. Almeida. *Inorg. Chem. Commun.*, **6**, 565 (2003).

[24] L. Pilia, C. Faulmann, I. Malfant, V. Collière, M.L. Mercuri, P. Deplano, P. Cassoux. *Acta Crystallogr., Sect. C: Cryst. Struct. Commun.*, **58**, m240 (2002).

[25] H. Yamochi, N. Sogoshi, Y. Simizu, G. Saito, K. Matsumoto. *J. Mater. Chem.*, **11**, 2216 (2001).

[26] S. Schenk, I. Hawkins, S.B. Wilkes, A.E. Underhill, A. Kobayashi, H. Kobayaschi. *Chem. Commun.*, 1648 (1993).

[27] O.A. Dyachenko, S.V. Konovalikhin, A.I. Kotov, G.V. Shilov, E.B. Yagubskii, C. Faulmann, P. Cassoux. *Chem. Commun.*, 508 (1993).

[28] P. Deplano, L. Leoni, M.L. Laura Mercuri, J.A. Schlueter, U. Geiser, H.H. Wang, A.M. Kini, J.L. Manson, C.J. Gómez-García, E. Coronado, H.-J. Koo, M.-H. Whangbo. *J. Mater. Chem.*, **12**, 3570 (2002).

[29] K. Awaga, T. Okuno, Y. Maruyama, A. Kobayashi, H. Kobayashi, S. Schenk, A.E. Underhill. *Inorg. Chem.*, **33**, 5598 (1994).

[30] S. Curreli, P. Deplano, M.L. Mercuri, L. Pilia, A. Serpe, J.A. Schlueter, M.A. Whited, U. Geiser, E. Coronado, C.J. Gómez-García, E. Canadell. *Inorg. Chem.*, **43**, 2049 (2004).

[31] Y. Journaux, O. Kahn. *Dalton Trans.*, 1575 (1979).

[32] J. Ribas, A. Escuer, M. Monfort, R. Vicente, R. Cortés, L. Lezama, T. Rojo. *Coord. Chem. Rev.*, **193–195**, 1027 (1999).

[33] P.K. Dhara, S. Sarkar, M.G.B. Drew, M. Nethaji, P. Chattopadhyay. *Polyhedron*, **27**, 2447 (2008).

[34] C.G. Pierpont, D.N. Hendrickson, D.M. Duggan, F. Wagner, E.K. Barefield. *Inorg. Chem.*, **14**, 604 (1975).

[35] W. Xu, Q. Fang, G. Xue, W.-T. Yu, G.-Q. Liu, D.-Q. Zhang, W. Xu, C.-Y. Xu, J.-B. Zhang. *Acta Chim. Sinica*, **60**, 2153 (2002).

[36] M.J. Frisch, G.W. Trucks, H.B. Schlegel, G.E. Scuseria, M.A. Robb, J.R. Cheesman, J.A. Montgomery Jr., T. Vreven, K.N. Kudin, J.C. Burant, J.M. Millam, S.S. Iyengar, J. Tomasi, V. Barone, B. Mennucci, M. Cossi, G. Scalmani, G.A. Petersson, H. Nakatsuji, M. Hada, M. Ehara, K. Toyota, R. Fukuda, J. Hasegawa, M. Ishoda, T. Nakajima, Y. Honda, O. Kitao, H. Nakai, M. Klene, X. Li, J.E. Knox, H.P. Hratchian, J.B. Cross, C. Adamo, J. Jaramillo, R. Gomperts, R.E. Stratmann, O. Yazyev, A.J. Austin, R. Cammi, C. Pomelli, J. Otcherski, P.Y. Ayala, K. Morokuma, G.A. Voth, P. Salvador, J.J. Danneberg, V.G. Zakrzewski, S. Dapprich, A.D. Daniels, M.C. Strain, O. Farkas, D.K. Malick, A.D. Rabuck, K. Raghavachari, J.B. Foresman, J.V. Ortiz, Q. Cui, A. Baboul, S. Clifford, J. Cioslowski, B.B. Stefanov, G. Liu, A. Liashenko, P. Piskorz, I. Kamaromi, L.R. Martin, D.J. Fox, T. Keith, M.A. Al-Laham, C.Y. Peng, A. Nanaykkara, M. Challacombe, P.M.W. Gill, B. Johnson, W. Chen, M.W. Wong, G. Gonzalez, J.A. Pople. *Gaussian 03, Revison B.03*, Gaussian Inc., Pittsburgh, PA (2003).

[37] L. Noodleman. *J. Chem. Phys.*, **74**, 5737 (1981).

[38] L. Noodleman, E.J. Baerends. *J. Am. Chem. Soc.*, **106**, 2316 (1984).

[39] L. Noodleman, D.A. Case. *Adv. Inorg. Chem.*, **38**, 423 (1992).

[40] F. Neese. An Ab Initio, DFT and Semiempirical electronic structure package, Program Version 2.7, Revision 0; Lehrstuhl fuer Theoretische Chemie Institut fuer Physikalische und Theoretische Chemie, Universitaet Bonn, Germany, 20 January (2010).

[41] A.D. Becke. *J. Chem. Phys.*, **98**, 5648 (1993).

[42] A.D. Becke. *Phys. Rev. A*, **38**, 3098 (1988).

[43] C. Lee, W. Yang, R.G. Parr. *Phys. Rev. B*, **37**, 785 (1988).

[44] A. Schäfer, H. Horn, R. Ahlrichs, *J. Chem. Phys.*, **97**, 2571 (1992).

[45] F. Weigend, R. Ahlrichs. *Phys. Chem. Chem. Phys.*, **7**, 3297 (2005).

[46] N. Robertson, L. Cronin. *Coord. Chem. Rev.*, **227**, 93 (2002).

[47] Y.-H. Chi, J.-M. Shi, H.-N. Li, W. Wei, E. Cottrill, N. Pan, H. Chen, Y. Liang, L. Yu, Y.-Q. Zhang, C. Hou. *Dalton Trans.*, **42**, 15559 (2013).